[Supplementary Materials]

Title: Spatial scale-dependent land-atmospheric methane exchange in the northern high latitudes from 1993 to 2004

Authors: X. Zhu[1], Q. Zhuang[1,2], X. Lu[3], and L. Song[1,4,5]

[1]Department of Earth, Atmospheric and Planetary Sciences, Purdue University, West Lafayette, IN, 47907, USA

[2]Department of Agronomy, Purdue University, West Lafayette, IN 47907, USA

[3]The Ecosystems Center, Marine Biological Laboratory, Woods Hole, MA 02543, USA

[4]Institute of Geographic Sciences and Natural Resources Research, Chinese Academy of Sciences, Beijing, 100101, China

[5]Graduate University of the Chinese Academy of Sciences, Beijing, 100049, China

Corresponding author: X. Zhu, Department of Earth, Atmospheric and Planetary Sciences, Purdue University, West Lafayette, IN, 47907, USA. Email: zhu123@purdue.edu

(Submitted to *Biogeosciences*)

TOPMODEL parameterization scheme

An illustration of the TOPMODEL-based parameterization scheme was shown in Fig. S3. Watershed-mean topographic wetness index (TWI) (Fig. S3b) was calculated from original TWI data (Fig. S3a) according to basin boundaries from watershed delineation (Fig. S2). Time-varying scaling parameter m (m values of July in 1994 are shown in Fig. S3c) was estimated from Eq. (3) and Eq. (4).The topography-related data, including TWI, watershed delineation and terrain slope, was acquired from HYDRO1K database (http://eros.usgs.gov/#Find_Data/Products_and_Data_Available/gtopo30/hydro), which provides global coverage of topographically derived data based on 30-sec USGS-GTOPO30 DEM data. The original five-level watershed delineation basin data was aggregated into four-level data according to Pfafstetter code (http://eros.usgs.gov/#/Find_Data/Products_and_Data_Available/gtopo30/hydro/P311), with average surface area of 6597 km^2 (Fig. S2).

The calibrated time-varying α in Eq. (3) were shown in Fig. S4a, and the comparison of total inundated area from satellite observations and model simulation were shown in Fig. S4b. The calibrated parameter α had a strong temporal variation: larger in warmer seasons and smaller in colder seasons. The monthly parameter α was spatially constant and larger α corresponded to larger parameter m, and resulted in higher variance of local WTD. It is important to note that, in our three-step calibration procedure, only the total inundated area over the whole region, rather than for each grid cell, was confirmed by satellite data. The calibration at each grid cell was impossible since only inundated area fraction data (for West Siberian Lowlands, ~7% of all grid cells were inundated during the growing season (Fig. 4)) rather than WTD data was available from satellite observations.

References

Bellisario, L. M., Bubier, J. L., Moore, T. R., and Chanton, J. P.: Controls on CH_4 emissions from a northern peatland, Glob. Biogeochem. Cycles, 13, 81-91, 1999.

Christensen, T. R.: Methane emission from Arctic tundra, Biogeochem., 21, 117-139, 1993.

Fan, Y., Li, H., and Miguez-Macho, G.: Global Patterns of Groundwater Table Depth, Science, 339, 940-943, 2013.

Glagolev, M., Kleptsova, I., Filippov, I., Maksyutov, S., and Machida, T.: Regional methane emission from West Siberia mire landscapes, Environ. Res. Lett., 6, 045214, 2011.

Heyer, J., Berger, U., Kuzin, I. L., and Yakovlev, O. N.: Methane emissions from different ecosystem structures of the subarctic tundra in Western Siberia during midsummer and during the thawing period, Tellus B, 54, 231-249, 2002.

Moore, T. R., Heyes, A., and Roulet, N. T.: Methane emissions from wetlands, southern Hudson Bay lowland, J. Geophys. Res., 99, 1455-1467, 1994.

Moosavi, S. C., Crill, P. M., Pullman, E. R., Funk, D. W., and Peterson, K. M.: Controls on CH_4 flux from an Alaskan boreal wetland, Glob. Biogeochem. Cycles, 10, 287-296, 1996.

Nakano, T., Kuniyoshi, S., and Fukuda, M.: Temporal variation in methane emission from tundra wetlands in a permafrost area, northeastern Siberia, Atmos. Environ., 34, 1205-1213, 2000.

Rhew, R. C., Teh, Y. A., and Abel, T.: Methyl halide and methane fluxes in the northern Alaskan coastal tundra, J. Geophys. Res., 112, G02009, 2007.

Sachs, T., Giebels, M., Boike, J., and Kutzbach, L.: Environmental controls on CH_4 emission from polygonal tundra on the microsite scale in the Lena river delta, Siberia, Glob. Change Biol., 16, 3096-3110, 10.1111/j.1365-2486.2010.02232.x, 2010.

Turetsky, M. R., Wieder, R. K., and Vitt, D. H.: Boreal peatland C fluxes under varying permafrost regimes, Soil Biol. Biochem., 34, 907-912, 2002.

Vourlitis, G. L., Oechel, W. C., Hastings, S. J., and Jenkins, M. A.: A system for measuring in situ CO_2 and CH_4 flux in unmanaged ecosystems: an arctic example, Funct. Ecol., 369-379, 1993.

Table S1 Description of the site methane measurements made in the pan-Arctic reported by published literatures

Site name	CH_4 flux range (mean) ($mg\ CH_4\ m^{-2}\ d^{-1}$)	Reference
Toolik Lake, Alaska, USA	0.6 ~ 42.8 (17.5)	Christensen (1993)
Toolik Lake, Alaska, USA	22.7 ~ 112.4 (65.6)	Christensen (1993)
Patuanak, Saskatchewan, Canada	0.0 ~ 0.3 (0.1)	Turetsky et al. (2002)
Yamal Peninsula, Russia	4.3 ~ 195.3 (83.5)	Heyer et al. (2002)
Chersky, Russia	-0.7 ~ 281.0 (81.8)	Nakano et al. (2000)
Lena Delta, Russia	7.7 ~ 94.0 (50.9)	Sachs et al. (2010)
Thompson, Manitoba, Canada	19.7 ~ 226.0 (89.0)	Bellisario et al. (1999)
North Point - Kinosheo transect, Hudson Bay lowlands, Canada	1.0 ~ 16.4 (6.6)	Moore et al. (1994)
North Point - Kinosheo transect, Hudson Bay lowlands, Canada	2.7 ~ 104.7 (25.6)	Moore et al. (1994)
Lementa Bog, Fairbanks, Alaska, USA	0.0 ~ 57.3 (28.6)	Moosavi et al. (1996)
Prudhoe Bay, Alaska, USA	95.0 ~ 185.0 (140.0)	Vourlitis et al. (1993)
Barrow, Alaska, USA	10.0 ~ 67.0 (45.3)	Rhew et al. (2007)
Tobolsk, West Siberia, Russia	-2.7 ~ 115.0 (30.0)	Glagolev et al. (2011)
Surgut, West Siberia, Russia	-2.0 ~ 310.2 (34.6)	Glagolev et al. (2011)
Pangody, West Siberia, Russia	-1.5 ~ 468.0 (87.8)	Glagolev et al. (2011)
Plotnikovo, West Siberia, Russia	-9 ~ 471.0 (174.8)	Glagolev et al. (2011)
Noyabrsk-Hills, West Siberia, Russia	-2.3 ~ 110.5 (41.4)	Glagolev et al. (2011)
Noyabrsk-Palsa, West Siberia, Russia	-0.6 ~ 371.3 (140.2)	Glagolev et al. (2011)
Vah, West Siberia, Russia	20.7 ~ 246.2 (114.8)	Glagolev et al. (2011)
Muhrino, West Siberia, Russia	-7.2 ~ 428.2 (63.0)	Glagolev et al. (2011)
Tazovsky, West Siberia, Russia	-6.2 ~ 213.6 (34.3)	Glagolev et al. (2011)
Gyda, West Siberia, Russia	-0.5 ~ 156.9 (25.2)	Glagolev et al. (2011)
Skala, West Siberia, Russia	0.0 ~ 4.3 (2.7)	Glagolev et al. (2011)

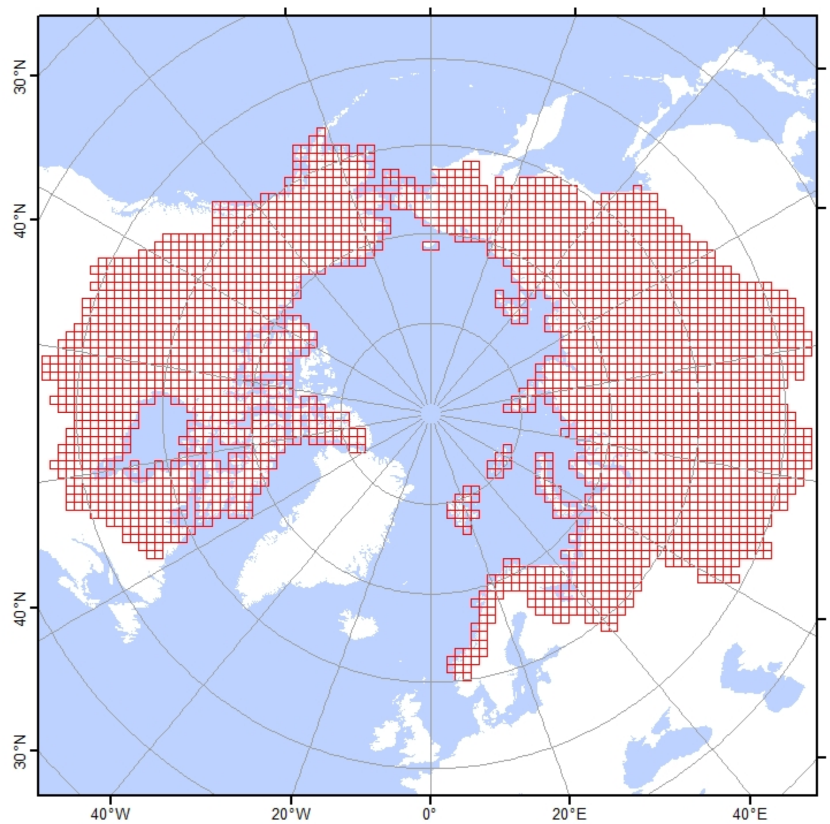

Fig. S1. The VIC grid cells over the pan-Arctic at a spatial resolution of 100 km.

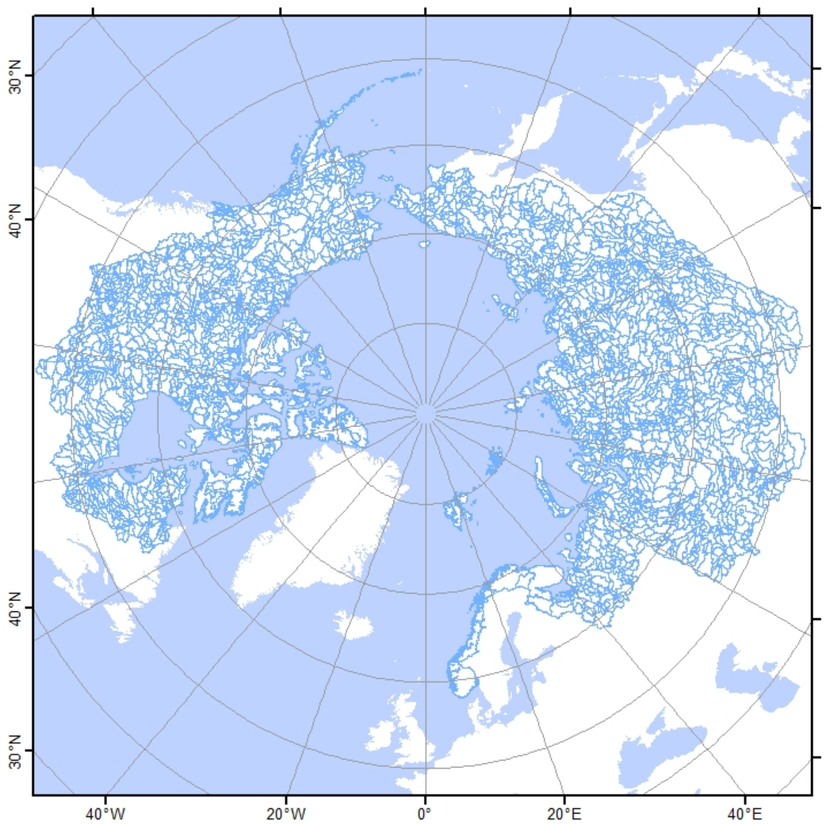

Fig. S2. The delineation of the watersheds over the pan-Arctic (average surface area of 6597 km^2), derived from HYDRO1K dataset.

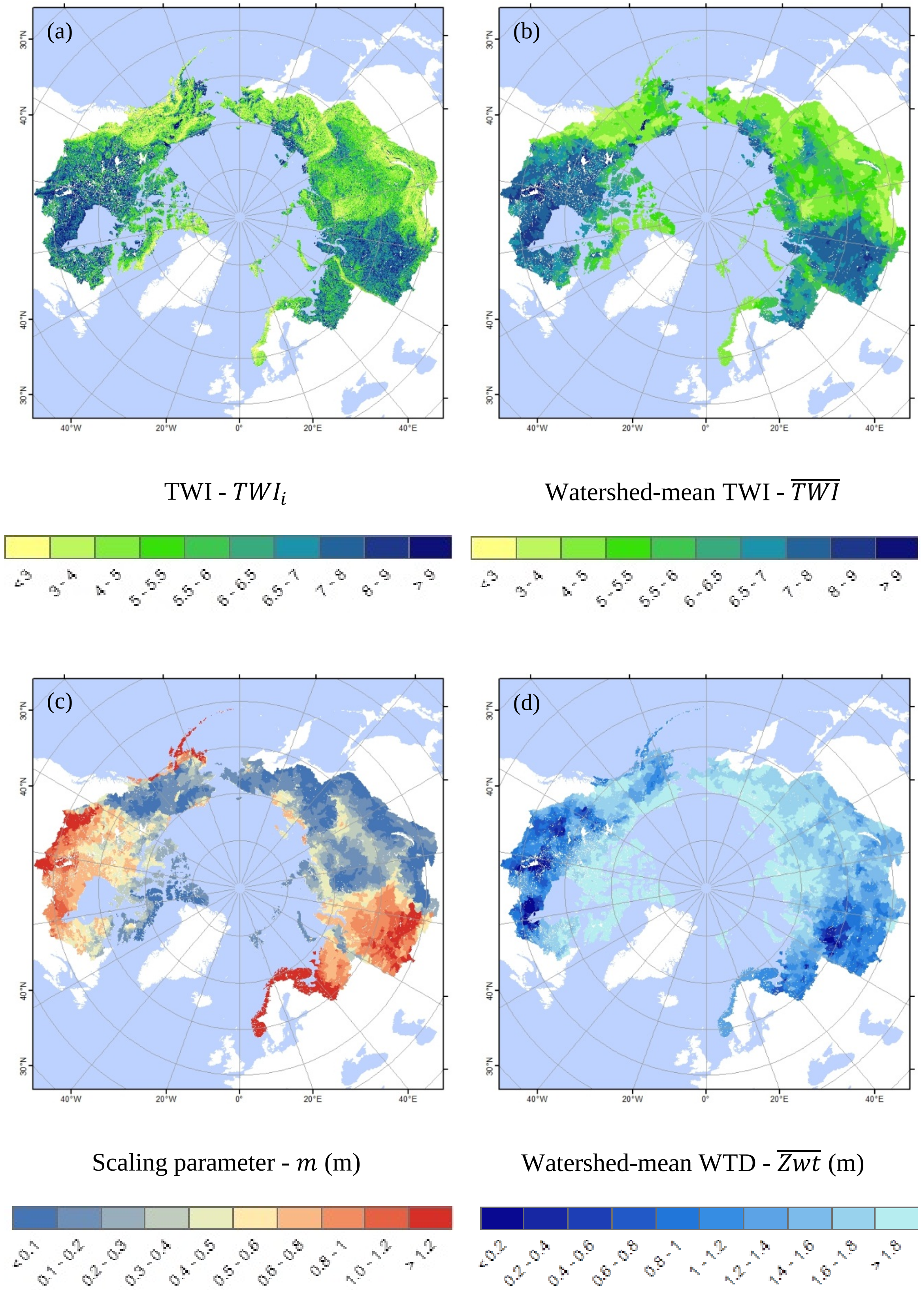
(a)
(b)
(c)
(d)
30°N
40°N
40°W
20°W
0°
20°E
40°E
TWI - TWI_i
Watershed-mean TWI - $\overline{TWI}$
<3
3 - 4
4 - 5
5 - 5.5
5.5 - 6
6 - 6.5
6.5 - 7
7 - 8
8 - 9
> 9
Scaling parameter - m (m)
Watershed-mean WTD - $\overline{Zwt}$ (m)
<0.1
0.1 - 0.2
0.2 - 0.3
0.3 - 0.4
0.4 - 0.5
0.5 - 0.6
0.6 - 0.8
0.8 - 1
1.0 - 1.2
> 1.2
<0.2
0.2 - 0.4
0.4 - 0.6
0.6 - 0.8
0.8 - 1
1 - 1.2
1.2 - 1.4
1.4 - 1.6
1.6 - 1.8
> 1.8

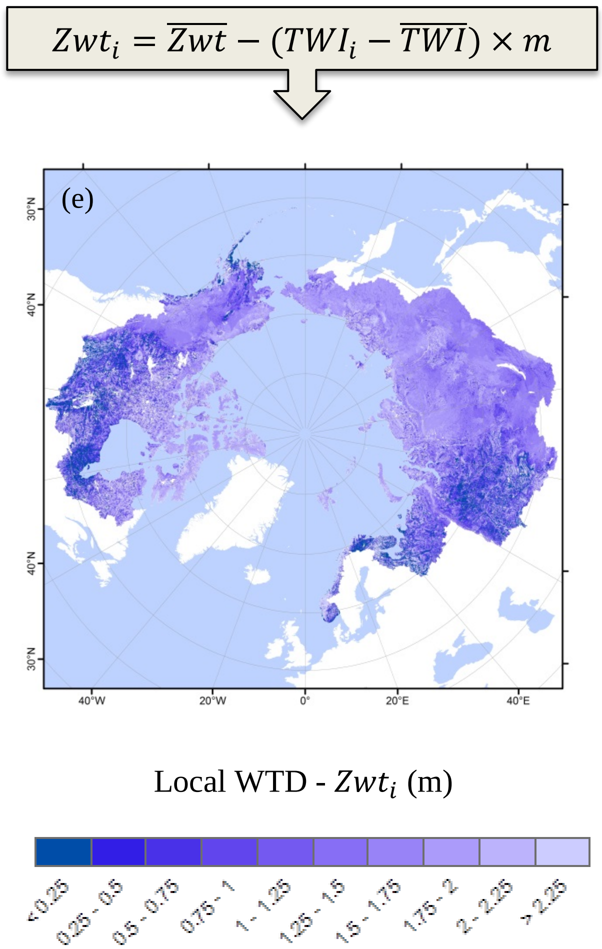

Fig. S3. An illustration of TOPMODEL-based parameterization scheme used for redistributing water table depth. See text for more details.

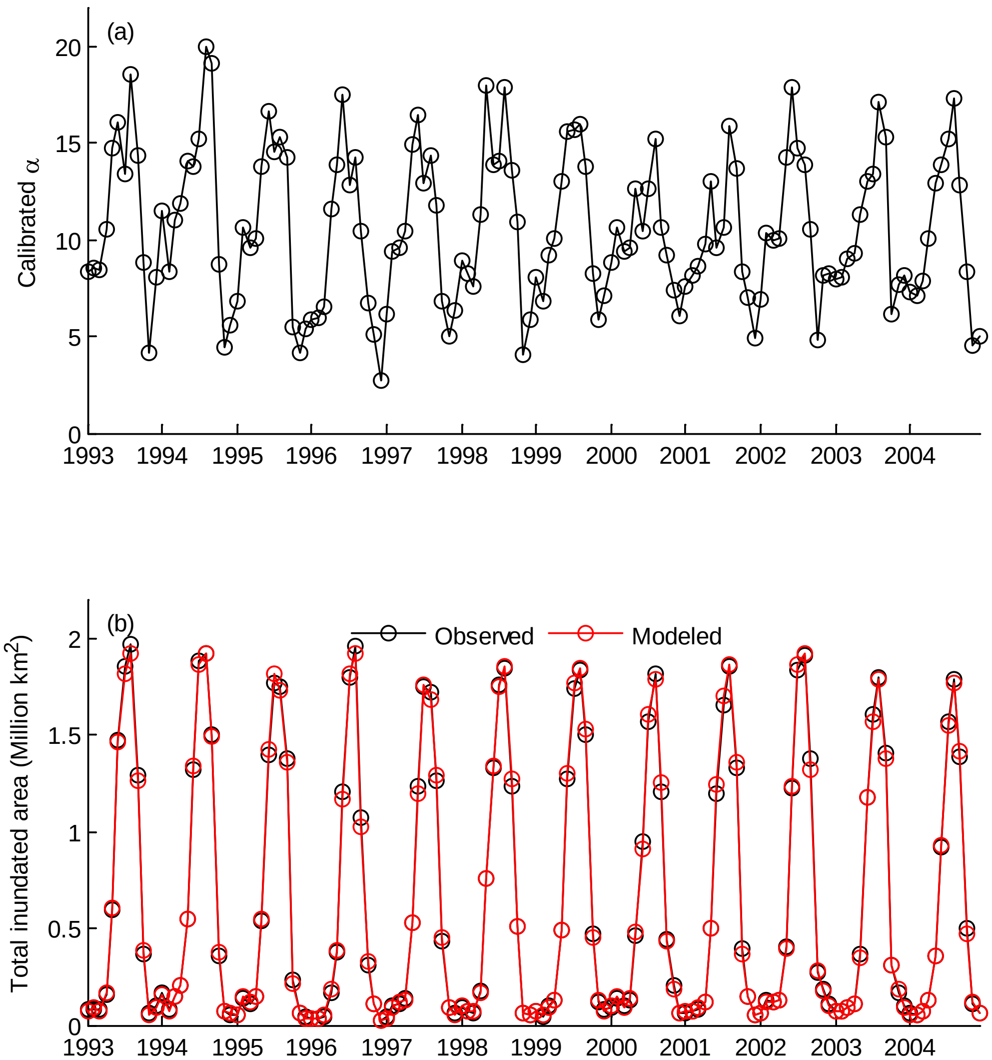

Fig. S4. Calibrated monthly parameter α for TOPMODEL-based parameterization (a) and the comparison of monthly total inundated area from satellite observations and model simulations (b) from 1993 to 2004.

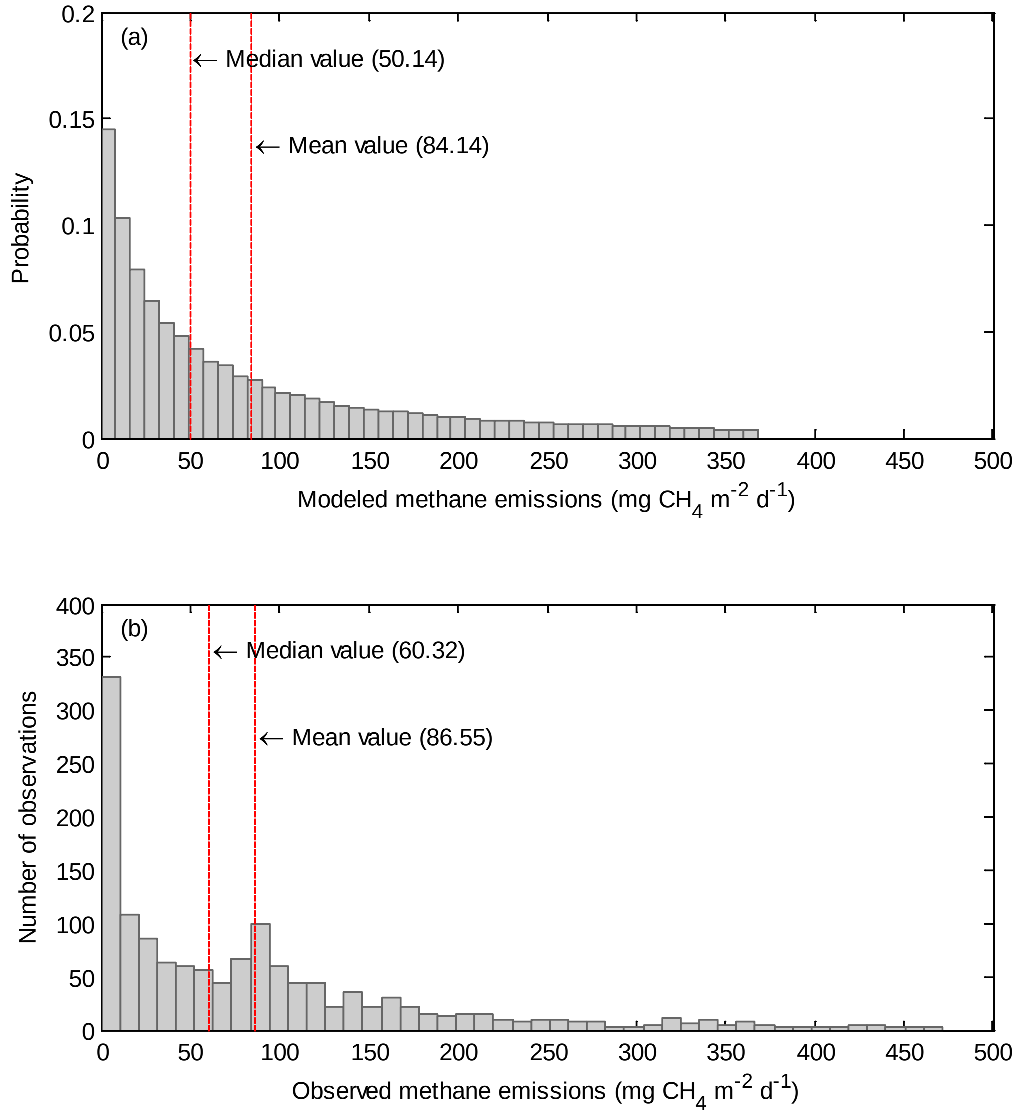

Fig. S5. Probability distribution of modeled (at a 5-km spatial resolution) (a) and observed (b) mean methane emissions during the growing season (May - Sep.) across West Siberian Lowlands.

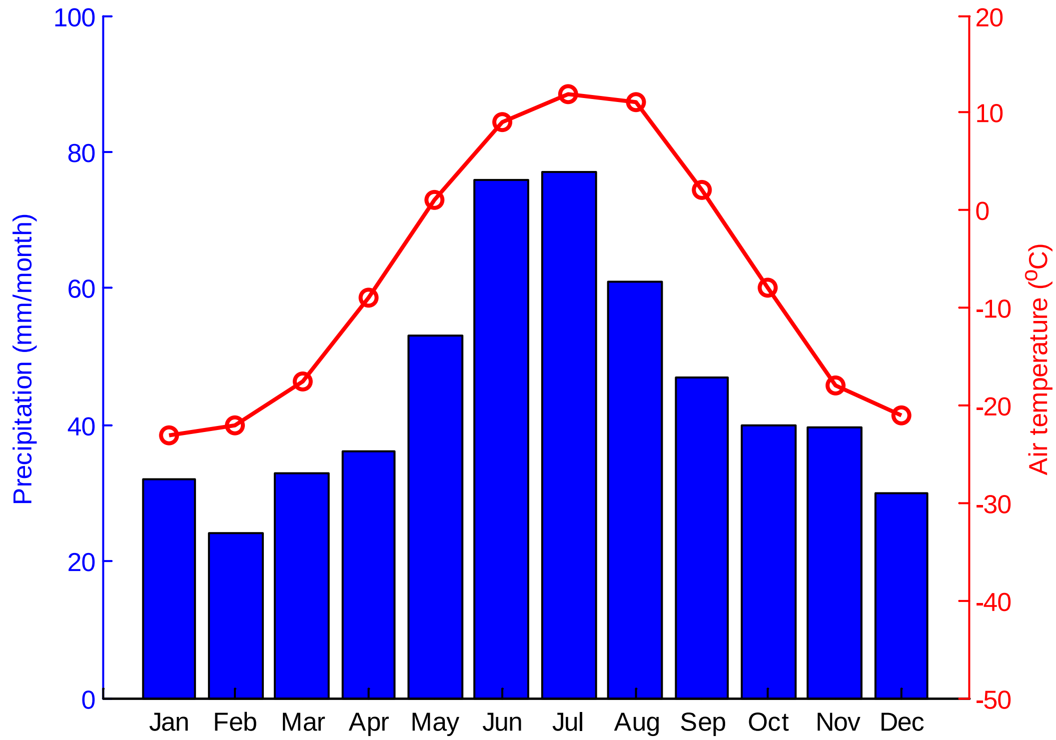

Fig. S6. Monthly precipitation and air temperature averaged over the pan-Arctic for the year 1994 (maximum methane emission year from 1993 to 2004 at a 5-km spatial resolution). The climate data were derived from NCEP/NCAR Reanalysis dataset.

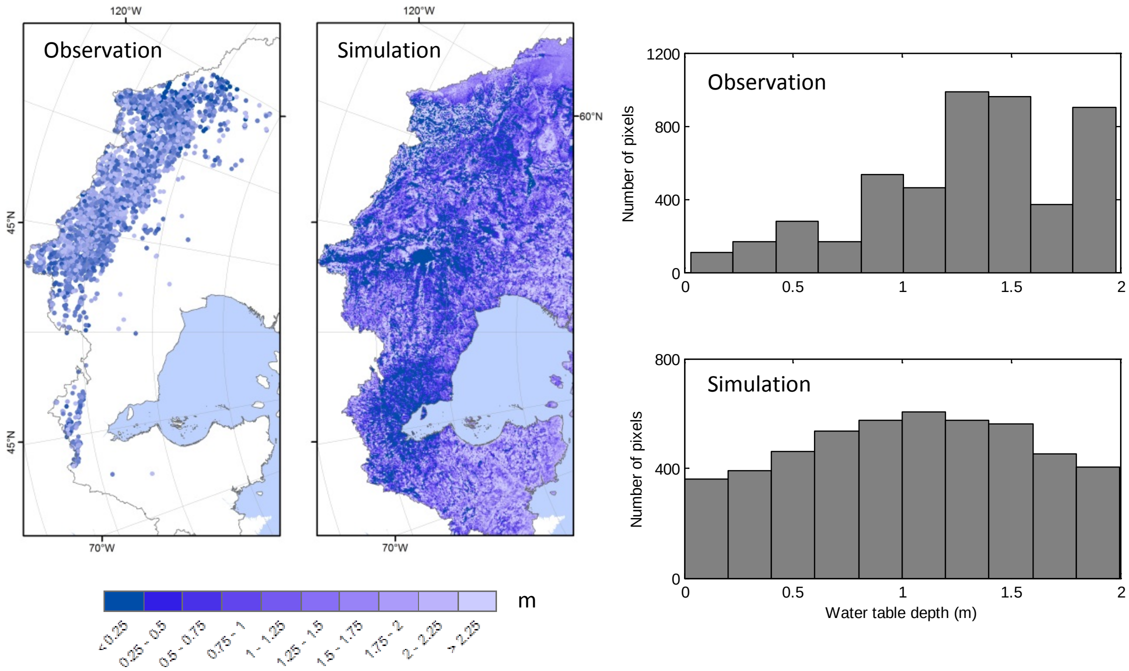

Fig. S7. Comparison of observed and simulated water table depth during the growing season (May - Sep.) across southern Canada. Observed water table depths at well sites (~5000, first gridded into 5-km cells) are retrieved from Fan et al., 2013. Only those well sites with shallow water table (< 2 m below the land surface) are included in our comparison.